

Kramers-Kronig relations and high-order nonlinear susceptibilities

Carsten Brée

*Weierstraß-Institut für Angewandte Analysis und Stochastik, D-10117 Berlin, Germany and
Max-Born-Institut für Nichtlineare Optik und Kurzzeitspektroskopie, D-12489 Berlin, Germany*

Ayhan Demircan

Invalidenstraße 114, D-10115 Berlin, Germany

Günter Steinmeyer

*Optoelectronics Research Centre, Tampere University of Technology, 33101 Tampere, Finland and
Max-Born-Institut für Nichtlineare Optik und Kurzzeitspektroskopie, D-12489 Berlin, Germany*

(Received 27 September 2011; published 12 March 2012)

As previous theoretical results recently revealed, a Kramers-Kronig transform of multiphoton absorption rates allows for a precise prediction on the dispersion of the nonlinear refractive index n_2 in the near infrared. It was shown that this method allows reproduction of recent experimental results on the importance of the higher-order Kerr effect. Extending these results, the current manuscript provides the dispersion of n_2 for all noble gases in excellent agreement with reference data. It is furthermore established that the saturation and inversion of the nonlinear refractive index is highly dispersive with wavelength, which indicates the existence of different filamentation regimes. While shorter laser wavelengths favor the well-established plasma clamping regime, the influence of the higher-order Kerr effect (HOKE) dominates in the long-wavelength regime.

DOI: [10.1103/PhysRevA.85.033806](https://doi.org/10.1103/PhysRevA.85.033806)

PACS number(s): 42.65.An, 42.65.Jx, 42.65.Hw

I. INTRODUCTION

The optical nonlinearity of atomic and molecular gases is of paramount importance in high-field physics [1], for high-order harmonic generation [2], attosecond pulse generation [3], hollow-fiber compression [4], and the formation of filaments [5]. The nonlinear optical effect of self-phase modulation is the key mechanism for obtaining spectral broadening in optical compression schemes [6]. Until recently, such pulse compression was the only possible way for generating sub-10-fs pulses with hundreds of microjoule pulse energy, using noble gases in hollow fibers or filaments [7]. This combination of pulse energy and shortness is a requirement for subsequent attosecond pulse generation. Only recently, this approach was challenged by chirped pulse optical parametric amplification [8]. In this light, it is remarkable that our knowledge of numerical values of the nonlinear refractive index n_2 rests on only few direct measurements (see [9,10] and references therein), most of which have been conducted in the 800–1000 nm range. Even for the relatively well established and technologically highly important case of argon, one can find a two-order-of-magnitude spread of quoted values for n_2 in literature, reaching from 0.12 to 19×10^{-19} cm²/W [9,11]. Moreover, recent advances in laser technology enable the use of gas-based compression, filamentation, and supercontinuum generation schemes, in the midinfrared [12] as well as in the ultraviolet [13]. Traditionally, wavelength scaling of n_2 has utilized variants of Miller's formulas [14]. Again, differing scaling laws are suggested in literature [10,15], and the reliability of such extrapolations is disputable [16], in particular for predicting dependable n_2 values in the ultraviolet.

Here we extend the alternative approach of Ref. [17] for computing refractive index values of noble gases. Our approach is based on a Kramers-Kronig (KK) transform [18,19] of multiphoton absorption rates [20]. Requiring only

knowledge of the ionization energy of the gas, the full spectral dependence $n_2(\omega)$ can be computed, including the expected sign change of n_2 beyond the two-photon resonance. Moreover, our formalism also allows for computation of higher-order contributions $n_4 I^2, n_6 I^3$, etc. to the refractive index,

$$n(I) = \sum_{k \geq 0} n_{2k} I^k, \quad (1)$$

and enables a comparison of our theoretical results on the intensity-dependent refractive index (IDRI) to recent measurements [21]. In addition, we investigate the IDRI of all noble gases as well as the wavelength dependence of the Kerr saturation. In light of new applications in previously inaccessible wavelength ranges, this gives rise to important conclusions concerning the formation of filaments in the absence of dissipative ionization effects.

II. KRAMERS-KRONIG RELATIONS IN NONLINEAR OPTICS

Nonlinear optical Kramers-Kronig relations [22] are a straightforward generalization of the well-examined linear optical case [23,24]. In the time domain, any order $P^{(n)}(t)$ of the electric-field-induced polarization

$$P(t) = P^{(1)}(t) + P^{(2)}(t) + P^{(3)}(t) + \dots \quad (2)$$

is assumed to be mediated by temporal response kernels $R^{(n)}(\tau_1, \dots, \tau_n)$. Thus causality requires $R^{(n)}(\tau_1, \dots, \tau_n) = R^{(n)}(\tau_1, \dots, \tau_n)\theta(\tau_i)$ to hold for any $i = 1, \dots, n$, where $\theta(\tau)$ is the Heaviside step function. In the frequency domain, this requirement immediately yields the KK relation for the complex nonlinear optical susceptibilities $\chi^{(n)}$,

$$\begin{aligned} \text{Re}\chi^{(n)}(-\omega_\sigma; \omega_1, \omega_2, \dots, \omega_i, \dots, \omega_n) \\ = \frac{2}{\pi} \text{P} \int_0^\infty \frac{\Omega \text{Im}\chi^{(n)}(-\omega_\sigma; \omega_1, \omega_2, \dots, \Omega, \dots, \omega_n)}{\Omega^2 - \omega_i^2} d\Omega, \quad (3) \end{aligned}$$

and the inverse KK relation

$$\begin{aligned} \text{Im}\chi^{(n)}(-\omega_\sigma; \omega_1, \omega_2, \dots, \omega_i, \dots, \omega_n) \\ = -\frac{2\omega_i}{\pi} \text{P} \int_0^\infty \frac{\text{Re}\chi^{(n)}(-\omega_\sigma; \omega_1, \omega_2, \dots, \Omega, \dots, \omega_n)}{\Omega^2 - \omega_i^2} d\Omega, \end{aligned} \quad (4)$$

where P denotes the Cauchy principal value. An alternative, yet equivalent form of the KK relation was introduced by Sheik-Bahae *et al.* to compute the nonlinear refractive index $\sim \text{Re}\chi^{(3)}$ from the two-photon absorption (TPA) coefficients for wide-band-gap semiconductors [18,19]. This formulation resembles that of the linear optical KK relations and relates refractive index changes $\Delta n(\omega; \xi)$ induced by some perturbation to the corresponding change of absorption $\Delta\alpha(\omega; \xi)$ in the following way:

$$\Delta n(\omega; \xi) = \frac{c}{\pi} \text{P} \int_0^\infty \frac{\Delta\alpha(\Omega; \xi)}{\Omega^2 - \omega^2} d\Omega. \quad (5)$$

Here, the parameter ξ quantifies the physical cause of the refractive index change. For example, the cause may be given by an intense pump beam of frequency ω_2 . In this case, setting $\omega = \omega_1$ and $\xi = \omega_2$ in Eq. (5) yields the index change $\Delta n(\omega_1; \omega_2)$ responsible for cross-phase modulation. From the KK relations, one concludes that this index change is related to an absorption change $\Delta\alpha(\omega_1; \omega_2)$ from nondegenerate TPA of photons with frequencies ω_1 and ω_2 . For a pump beam of intensity I_2 and frequency ω_2 , this quantity scales linearly with I_2 according to

$$\Delta\alpha(\omega_1; \omega_2) = \beta_2(\omega_1; \omega_2) I_2, \quad (6)$$

as does the nonlinear index change

$$\Delta n(\omega_1; \omega_2) = n_2(\omega_1; \omega_2) I_2. \quad (7)$$

The coefficient β_2 relates to the TPA cross section σ_2 and Eq. (6) can be rewritten as $w = \sigma_2(\omega_1, \omega_2) I_1 I_2$. The absorption rate w describes optical field-induced two-photon transition from the valence to the conduction band of the optical medium. Analytical expressions for the nondegenerate TPA coefficient $\beta_2(\omega_1; \omega_2)$ were derived in Refs. [19,25]. A reasonable approximation [17,18] of the nondegenerate TPA coefficient used in Eq. (5) is provided by the expression

$$\beta_2(\omega_1; \omega_2) = \overline{\beta_2} \left(\frac{\omega_1 + \omega_2}{2} \right), \quad (8)$$

where $\overline{\beta_2}(\omega)$ is the TPA coefficient for simultaneous absorption of photons of equal frequencies.

III. APPLICATION TO NONLINEAR SUSCEPTIBILITIES OF NOBLE GASES

The very successful formalism developed by Sheik-Bahae *et al.* [18,19] and Hutchings *et al.* [22] encourages the examination of a possible generalization toward higher-order susceptibilities. In the perturbative regime of nonlinear optics, both the nonlinearly induced index change Δn and the

absorption change $\Delta\alpha$ can be expressed as a power series, i.e.,

$$\Delta n = \sum_{k>0} n_{2k} I^k, \quad \Delta\alpha = \sum_{K>1} \beta_K I^{K-1}. \quad (9)$$

For the degenerate case, we can set $\Delta n \equiv \Delta n(\omega)$ and $\Delta\alpha \equiv \Delta\alpha(\omega)$. Then the Kerr coefficients n_{2k} and the K -photon absorption coefficients β_K are related to the real and imaginary parts of the nonlinear optical susceptibilities $\chi^{(n)}$ according to

$$n_{2k} = \frac{2^{k-1} \mathcal{C}^{(k)}}{n_0 (n_0 \epsilon_0 c)^k} \text{Re}\chi^{(2k+1)}, \quad (10)$$

$$\beta_K = \frac{\omega_0}{c} \frac{2^{K-1} \mathcal{C}^{(K-1)}}{n_0 (n_0 \epsilon_0 c)^{(K-1)}} \text{Im}\chi^{(2K-1)}, \quad (11)$$

with a combinatorial factor

$$\mathcal{C}^{(k)} = \frac{(2k+1)!}{2^{2k} k! (k+1)!}. \quad (12)$$

Generalizing the results of Sheik-Bahae *et al.* to self-refraction in noble gases, we now seek for an appropriate KK relation that relates the Kerr coefficients of any given order K to multiphoton absorption (MPA) coefficients β_K . These coefficients are related to ionization cross sections σ_K via

$$\beta_K = K \rho_0 \hbar \omega \sigma_K, \quad (13)$$

where ρ_0 is the number density of neutral atoms. The cross section σ_K governs the ionization rate at a given optical intensity I according to $w(I) = \sigma_K I^K$. In general, a power-law dependence of the ionization rate in an intense optical field is justified only for large values of the Keldysh parameter $\gamma = \sqrt{U_i/2U_p}$ [26,27], which is conveniently written in terms of the ratio of the ionization potential U_i of the gas species and the ponderomotive potential of the ionized electrons U_p in the laser field. In the opposite case $\gamma \ll 1$, a perturbative description of multiphoton absorption ceases to exist. Instead, tunneling ionization prevails in this regime, which, to exponential accuracy, is governed by the nonperturbative expression $w(I) = \exp(-\theta/3E)$. Here, θ is the characteristic internal atomic field strength of the gas species, and the electric field E is related to the intensity according to $I = \epsilon_0 n_0 c |E|^2/2$. It follows that throughout this work, special care has to be taken to assure validity of a perturbative description of the relevant nonlinear optical processes.

Analytical expressions for the required multiphoton cross sections are extracted from the perturbative limit $\gamma \gg 1$ of a recently published refined Keldysh theory [20], which provides excellent results for the ionization rate w , both in the perturbative and the tunneling regime. For the K -photon cross sections, this model yields

$$\begin{aligned} \sigma_K(\omega) = \frac{2\sqrt{2}C^2}{\pi} (2e)^{2n_*} \left(\frac{e}{2}\right)^{2K} \omega_p^{-3K+1} \left(\frac{q_e^2}{\hbar m_e \epsilon_0 c}\right)^K \\ \times \left(\frac{\omega_p}{\omega}\right)^{2n_*+2K-(3/2)} \exp\left(-\frac{\omega_p}{\omega}\right) w_0 \left[\sqrt{2K - 2\frac{\omega_p}{\omega}}\right], \end{aligned} \quad (14)$$

where $\omega_p = U_i/\hbar$, ω is the optical frequency, q_e , and m_e denote electron charge and mass, respectively, and ϵ_0 is the

vacuum permittivity. The constant $C^2 = \frac{2^{2n_*-2}}{\Gamma^2(n_*+1)}$ is obtained from an asymptotic expansion of the ground-state atomic wavefunction, $n_* = \sqrt{\omega_H/\omega_p}$ is the effective principal quantum number, and $\hbar\omega_H \approx 13.6$ eV is the ground-state energy of atomic hydrogen.

We now set

$$\beta_K(\omega_1, \dots, \omega_K) = \bar{\beta}_K \left(\frac{\omega_1 + \dots + \omega_K}{K} \right). \quad (15)$$

This relation approximates the nondegenerate absorption coefficient β_K in terms of the degenerate coefficient $\bar{\beta}$, evaluated at the mean frequency. This is a straightforward generalization of Eq. (8) successfully employed in Refs. [18,19]. It stems from the fact that Kramers-Kronig relations can in general be formulated only for nondegenerate absorption coefficients $\Delta\alpha(\omega_1, \omega_2, \dots, \omega_K)$ describing the absorption of K photons of unequal frequencies. In fact, within Kramers-Kronig relations, the employed approximation appears uncritical due to the fact that the dominant contribution to the Kramers-Kronig integral Eq. (5) comes from the vicinity of the pole $(\Omega^2 - \omega^2)^{-1}$ at $\Omega \sim \omega$.

With this approximation, we obtain the generalized KK relation

$$n_{2k}(\omega) = \frac{\rho_0 \hbar c}{\pi} \text{P} \int_0^\infty (\Omega + k\omega) \frac{\sigma_{k+1}(\frac{\Omega+k\omega}{k+1})}{\Omega^2 - \omega^2} d\Omega \quad (16)$$

for the computation of the Kerr coefficients n_{2k} to any order.

IV. BENCHMARKING THE MODEL: SECOND-ORDER KERR EFFECT

In the following, let us first consider the case of an unsaturated nonlinear refraction, i.e., $k = 1$. Given that there are approximations in our treatment, we first provide proof for the validity of our approach to compute the nonlinear refractive index. For the noble gases considered here, a wide variety of independent experimental and theoretical reference data on the second-order Kerr coefficient $n_2(\omega)$ exist. Theoretical models mostly calculate the hyperpolarizability in the static limit $\omega \rightarrow 0$ and interpolate the various related $\chi^{(3)}$ effects from there. According to Ref. [15], for small ω the dispersion of n_2 follows a series expansion in $\omega_L^2 = \nu\omega^2$,

$$n_2(\omega) = n_2(0)(1 + A\omega_L^2 + B\omega_L^4 + \dots), \quad (17)$$

where ν assumes the values 12, 6, and 4 for third harmonic generation (THG), electric-field-induced second harmonic generation (ESHG), and degenerate four-wave mixing (DFWM), respectively. Furthermore, the far-infrared limit $n_2 \sim \chi^{(3)}(0;0,0,0)$ and the coefficient A do not depend on the nonlinear optical process under consideration. The above series is usually truncated after the fourth-order term, permitting reliable extrapolation throughout the infrared, yet with decreasing accuracy in the visible. Given that Eq. (17) is always positive, this scaling law is expected to fail in the vicinity of the two-photon resonance. For our benchmark, we will therefore concentrate on the very precise theoretical values in the infrared. We also compute the Kerr coefficients in the vicinity of K -photon edges, which we discuss in the subsequent section, cf. Fig. 3.

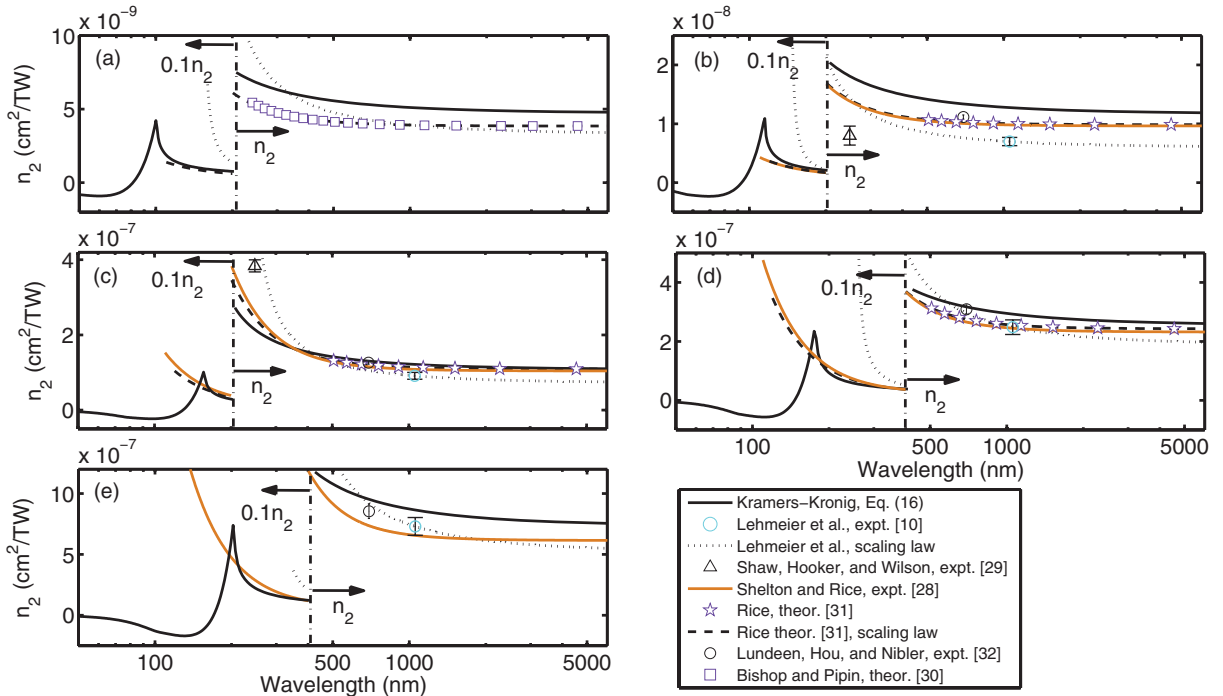


FIG. 1. (Color online) Off-resonant dispersion of n_2 for the noble gases (a) helium, (b) neon, (c) argon, (d) krypton, and (e) xenon. Solid lines: theoretical results derived from Kramers-Kronig transform Eq. (16). Dashed lines: experimental data of Ref. [28], scaled according to Eq. (17). Dotted lines: scaled Lehmeier data [10].

TABLE I. n_2 values in cm^2/TW for characteristic wavelength emitted by various laser materials. The number in brackets represents the power of 10.

	He	Ne	Ar	Kr	Xe
193 nm (ArF excimer)	7.8(-9)	2.2(-8)	3.1(-7)	1.0(-6)	4.2(-6)
248 nm (KrF excimer)	6.8(-9)	1.8(-8)	2.1(-7)	5.9(-7)	2.2(-6)
400 nm (Ti:sapph, SHG)	5.8(-9)	1.5(-8)	1.5(-7)	3.9(-7)	1.2(-6)
800 nm (Ti:sapph)	5.2(-9)	1.3(-8)	1.3(-7)	3.1(-7)	9.2(-7)
2000 nm (OPA)	4.9(-9)	1.2(-8)	1.1(-7)	2.7(-7)	8.0(-7)

Using Eq. (16) with $k = 1$ for the noble gases helium, neon, argon, krypton, and xenon, the solid lines Fig. 1 depict the resulting behavior of n_2 as a function of wavelength $\lambda = 2\pi c/\omega$. With ionization potentials $U_i = 24.59, 21.56, 15.76, 14.00$, and 12.13 eV for helium, neon, argon, krypton and xenon, the TPA edges for these gases are located at wavelengths $\lambda_{\text{TPA}} = 4\pi c/\omega_p = 101, 115, 157, 177$, and 204 nm, respectively. For comparison, the figures contain independent experimental data of Refs. [10,28,29]. The measured data of Ref. [28] were scaled to the considered λ range by fitting the data to a power series in $\nu\lambda^{-2}$, choosing $\nu = 4$ corresponding to DFWM. The theoretical data [30–32] in the chemical reference literature is obtained by a quantum mechanical sum-over-states ansatz. In the considered wavelength regime, our Eq. (16) deviates from the reference data by no more than 20%. Although our model calculations tend to slightly overestimate the reference data, the Kramers-Kronig approach yields excellent agreement with the reference data for argon and krypton, deviating by less than 10% from the reference data in the entire wavelength regime from 0.2 to 6 μm . Equation (3) in Ref. [10] represents an alternative wavelength scaling law and was used to scale the data obtained at 1.055 μm to the considered wavelength, cf. the dashed line in the subplots of Fig. 1. In addition, Table I shows n_2 values of the considered noble gases for characteristic laser frequencies of important laser-active materials. In the chemical reference literature, data on the $\chi^{(3)}$ nonlinearity mostly refers to microscopic polarizabilities rather than to macroscopic polarizations. Therefore we convert the macroscopic quantity n_2 to the third-order hyperpolarizability $\gamma^{(3)}$ using the Lorentz-Lorenz law. In the far-infrared limit, this yields the relation

$$\gamma^{(3)}(0) = \frac{8\epsilon_0^2 c}{\rho_0} n_2(0). \quad (18)$$

Our equation (16) predicts that for $\omega \rightarrow 0$, the value of n_2 is solely determined by the ionization potential U_i according to

$$\gamma^{(3)}(0) = \frac{64e^4 \hbar^2 \epsilon_0^2}{\omega_H^4 m_e^3} F(n_*). \quad (19)$$

Here the function $F(n_*)$ describes scaling of n_2 with the effective principal quantum number $n_* = \sqrt{\omega_H/\omega_p}$ of the gas species and is given by the integral representation

$$F(n_*) = \frac{(8e)^{2n_*}}{\Gamma^2(n_* + 1)} n_*^{10} \int_0^1 dx x^{2n_*+3/2} e^{-2x} w_0 [2\sqrt{1-x}]. \quad (20)$$

The variation of $\gamma^{(3)}(0)$ with the atomic ionization potential is shown as a dashed line in Fig. 2. The figure is supplemented

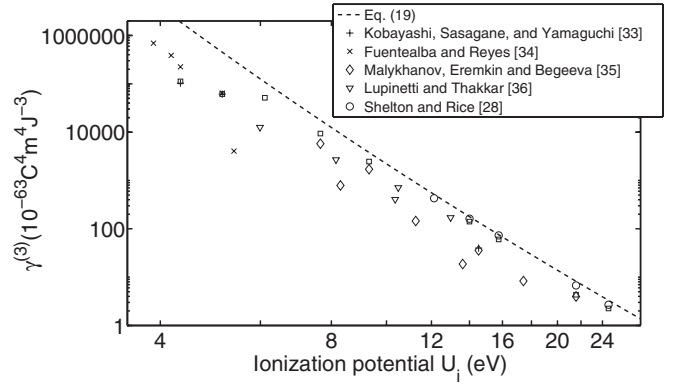


FIG. 2. Static limit of hyperpolarizability $\gamma^{(3)}(0)$ according to Eq. (19) versus ionization potential (dashed line). Theoretical reference data for various atomic species is taken from Refs. [28,33–36].

with independent measurements and calculations for various atomic species as performed in Refs. [28,33–36]. Our theory again yields excellent predictions for the noble gases. Except for the atomic species K, Li, B, and O, the predictions of our model for the long-wavelength limit of the third-order atomic hyperpolarizability of all considered atomic species coincide with independent calculations within one order of magnitude. Given that our theory is essentially a one-parameter theory, governed by the ionization potential, it disregards details in the atomic structure. Therefore this general order-of-magnitude agreement has to be considered as quite remarkable.

V. KERR SATURATION AND INVERSION

It has recently been shown, both experimentally and theoretically [17,21,37], that the Kerr refractive index of molecular and atomic gases may exhibit a saturation behavior. Given that a smooth transition from perturbative low-order harmonic generation to nonperturbative high-harmonic generation (HHG, [2]) with harmonic orders of hundred and above is experimentally observed, the very fact that $\chi^{(5)}$, $\chi^{(7)}$ effects, etc., play a role in nonlinear refraction at some elevated intensities may not appear overly surprising at first sight. Nevertheless, as plasma generation also results in a negative contribution to the refractive index, there is debate on which of these two effects sets in first, particularly in the generation of filaments [5]. Interestingly, high-harmonic generation has recently been observed during filamentary propagation [38], which provides further evidence that nonlinear susceptibilities of high order may play a long-underestimated role in filamentary propagation.

In order to observe saturation and inversion of the intensity-dependent refractive index, it is clearly a necessary condition that at least one of the higher-order Kerr coefficients n_{2k} be negative. Inspecting the well-understood scenario of two-photon induced nonlinear refraction, negative index contributions appear above the two-photon resonance $\omega_p/2$, analogous to the dispersion of linear refraction that turns to index values below 1 above the single-photon resonance ω_p . Therefore, quite generally, at a given wavelength λ one must expect that negative index contributions appear for orders k above $\lambda\omega_p/2\pi c$, which, for argon, implies a sign change to occur

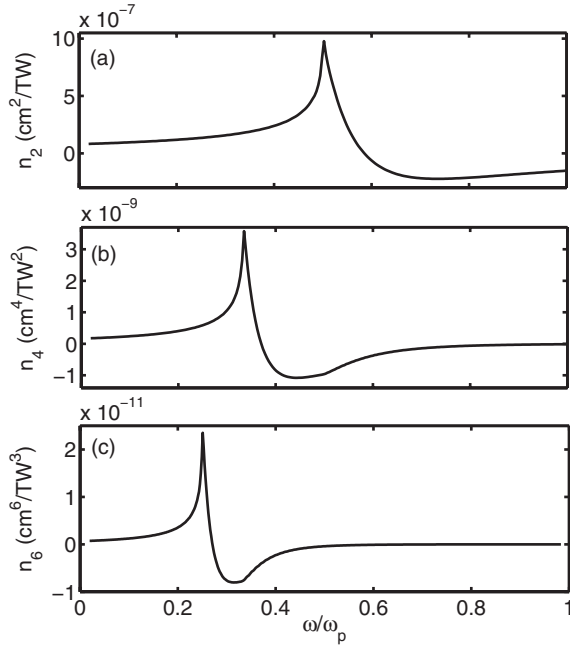


FIG. 3. Dispersion of (a) n_2 , (b) n_4 , and (c) n_6 for argon versus ω/ω_p in the vicinity of the $K = 2, 3$, and 4 photon resonance, respectively, as obtained from Eq. (16).

at n_{20} for $\lambda = 800$ nm. This behavior is exemplified by the dispersion of n_2, n_4 , and n_6 for argon shown in Fig. 3, as calculated by the generalized Kramers-Kronig relation [Eq. (16)] with $k = 1, 2$, and 3, respectively. As already exemplified for n_2 in the vicinity of the TPA resonance (Fig. 1), the higher-order coefficients n_4 and n_6 indeed show the expected behavior, yet with the resonance shifted toward lower frequencies $\omega_p/3$ and $\omega_p/4$, respectively. In fact, for arbitrary order and coefficients n_{2k} , the resonance is located at $\omega = \omega_p/(k + 1)$. Negative n_{2k} is observed for $\omega > \omega_p/(k + 1)$. Conversely, for a fixed frequency ω_0 , it follows that for $k > \omega_p/\omega - 1$, all Kerr coefficients $n_{2k}(\omega_0)$ are negative. By numerical evaluation of $\Delta n(I)$ for different noble gases, we now demonstrate our formalism. In particular, we relate the occurrence of the negative nonlinear refraction to the presence of the MPA resonances, which, in turn, give rise to the experimentally observed Kerr saturation and inversion. For the air constituents, i.e., argon, N_2 and O_2 , this procedure was already successfully applied [17] to reproduce the experimental results of Ref. [21]. We now extend this procedure to predict the onset of Kerr saturation for all other noble gases. The intensity-dependent refractive index for He, Ne, Kr, and Xe is plotted in Fig. 4. For comparison, the dashed lines represent the nonlinear refractive index according to the intensity clamping model of filamentation, $\Delta n = n_2 I + \rho/2\rho_c$. The inversion intensities I_{inv} for the considered noble gases, defined as the nontrivial root of

$$\sum n_{2k} I_{inv}^k = 0, \quad (21)$$

are contrasted to the clamping intensity, satisfying

$$n_2 I_c = \rho/2\rho_c \quad (22)$$

in Table II. Both intensities have been evaluated for a center wavelength of 800 nm. The plasma density entering the defi-

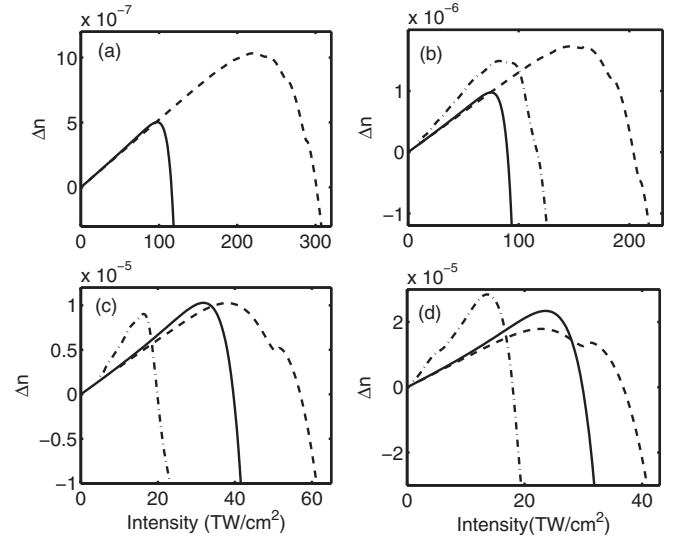


FIG. 4. Kerr saturation in (a) helium, (b) neon, (c) krypton, and (d) xenon at 800 nm due to higher-order Kerr terms [Eqs. (16) and (9), solid lines], classical filamentation model due to plasma clamping (dashed line), and TDSE results of Ref. [39] (dash-dotted lines).

nition of the clamping intensity is evaluated using a Gaussian temporal profile with FWHM duration of 90 fs, as was used in Ref. [21]. It is evident that saturation and inversion of the nonlinear refractive index occur at lower intensities than in the classical clamping model. Furthermore, this difference appears more pronounced with increasing ionization potential, as is especially obvious for helium [Fig. 4(a)]. In fact, a similar trend was previously reported theoretically in Ref. [39] with the help of numerical calculations of the time-dependent Schrödinger equation (TDSE). This finding already implies one important conclusion—the importance of the higher-order Kerr effect increases with the number of photons required to drive ionization. Therefore, filamentation in helium is more prone to Kerr-only filamentation than in xenon. The IDRI extracted from these calculations are shown as dash-dotted lines in Fig. 4.

The results discussed so far apply only for a center wavelength of 800 nm. However, as our model clearly shows, the n_{2k} coefficients exhibit a pronounced dispersion (Fig. 3), which is increasing with order. Therefore the inversion intensity I_{inv} , i.e., the point $\Delta n(I_{sat}) = 0$ at which higher-order Kerr effects neutralize the low-order contributions $n_2 I$, etc., to the refractive index should equally well show dispersion. Solving Eq. (21) for wavelengths in the range 350–1000 nm, the solid red curve in Fig. 5 depicts the solution $I_{inv}(\lambda)$ for the case of argon. The resulting trend is that the inversion intensity grows toward shorter wavelengths, with some local modulation on

TABLE II. Inversion intensity I_{inv} from saturation of the nonlinear refractive index versus clamping intensity I_c in the classical model of filamentation at 800 nm.

	Helium	Neon	Argon	Krypton	Xenon	O_2	N_2
I_{inv} (TW/cm ²)	113	89	49	40	30	36	50
I_c (TW/cm ²)	301	204	81	57	37	44	82

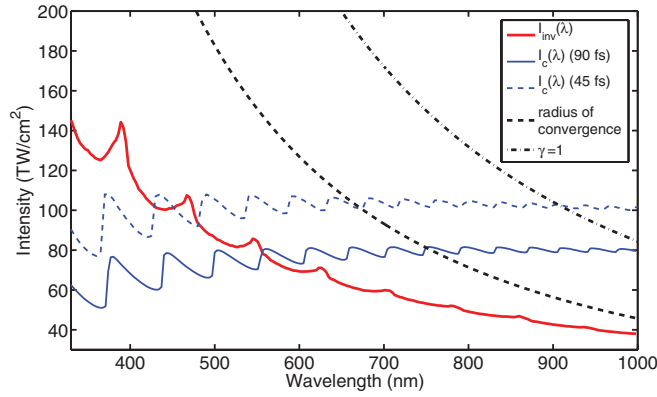


FIG. 5. (Color online) Inversion intensity due to higher-order Kerr effect versus wavelength (red solid line). Clamping intensity vs λ for 45-fs (solid blue) and 90-fs (dashed blue line) Gaussian pulses. Dashed black line: radius of convergence of series Eq. (9). Dash-dotted black line corresponds to $\gamma = 1$, separating the perturbative multiphoton regime from the nonperturbative tunneling regime.

top. Those local peaks are observed at $\lambda = (k + 1)2\pi c/\omega_p$, matching a $(k + 1)$ photon resonance.

Comparing the results of I_{inv} obtained from Eq. (16) with effects from ionization, we solve Eq. (22) in the wavelength range considered above. This allows us to obtain the wavelength dependence of the clamping intensity. In order to clarify the impact of pulse duration on the clamping intensity, the plasma density was evaluated for two different pulse durations. The results are represented by the blue solid (90-fs pulse) and the blue dashed (45-fs) curves in Fig. 5.

Figure 5 strongly suggests that, depending on the center wavelength of the employed laser system, there exist two different regimes of filamentation: the red and the blue solid lines representing $I_{\text{inv}}(\lambda)$ and $I_c(\lambda)$, respectively, intersect at roughly 560 nm. For shorter wavelengths, the clamping intensity is much smaller than the inversion intensity, which means that plasma formation prevails as the arresting mechanism in filament formation. For wavelengths above 600 nm, however, Kerr saturation appears to prevail, indicating the possibility of plasmaless formation of filaments. While it may be disputed where exactly this transition between plasma saturation and Kerr saturation will appear, our analysis clearly indicates the following important trends. Plasma-induced arrest of the beam collapse will always prevail in the ultraviolet, whereas Kerr-only-based filamentation scenarios are expected to prevail in the infrared. Moreover, there is a strong dependence on pulse duration. Few-cycle pulses are actually predicted to favor a higher-order Kerr arrest, whereas longer pulses favor the standard plasma scenario. In fact, concerning the dependence on wavelength and pulse duration, our results provide independent theoretical proof of the arguments of Ref. [40].

VI. LARGE- k ASYMPTOTICS AND RADIUS OF CONVERGENCE

Our discussion of the higher-order Kerr effects depends on a perturbative expansion of multiphoton laws. Quite

clearly, we therefore expect that our formalism will eventually collapse above a certain intensity. For this purpose, in order to investigate the limits of validity of our formalism, we investigate the limit of convergence of Eq. (9) as given by

$$I_{\text{conv}}(\omega) = \lim_{k \rightarrow \infty} \left| \frac{n_{2k}(\omega)}{n_{2k+2}(\omega)} \right|. \quad (23)$$

This expression directly implies the maximum intensity limit for which a perturbative description of nonlinear refraction does make sense. In fact, the asymptotic behavior of the Kerr coefficients for large k is given by the following completely analytic formula:

$$n_{2k}(\omega) \sim -D_k(\omega_p) \left(\frac{\omega_p}{\omega} \right)^{2n^*+2k+1/2} \exp\left(-\frac{\omega_p}{\omega}\right). \quad (24)$$

Therefore the coefficient $D_k(\omega_p)$, depending only on the ionization potential, is given by

$$D_k(\omega_p) = M \frac{\rho_0 \hbar c}{\pi^2} \sqrt{k} C^2 (2e)^{2n^*} \omega_p^{-3k-2} \times \left(\frac{e}{2} \right)^{2k+2} \left(\frac{q_e^2}{\hbar m_e \epsilon_0 c} \right)^{k+1} \quad (25)$$

with a numerical constant

$$M = \frac{1}{2} [\text{Ei}(2) - e^4 \text{Ei}(-2)] \approx 3.812, \quad (26)$$

and $\text{Ei}(x)$ denoting the well-known exponential integral [41]. With Eq. (25), it is straightforward to obtain the following expression for the radius of convergence:

$$I_{\text{conv}} = \frac{4 \hbar \omega_p m_e \epsilon_0 c}{e^2 q^2} \omega^2. \quad (27)$$

Interestingly, this equation may be recast into a condition on the Keldysh parameter γ , i.e., the series representation of the IDRI converges whenever

$$\gamma > e/2. \quad (28)$$

In the intensity-wavelength plane, the latter condition is represented by the dashed line shown in Fig. 5. Quite clearly, this condition is fulfilled in the entire near-infrared and visible wavelength range. Therefore we may conclude that our model holds for a relevant decision on the prevalence on plasma-based arrest vs Kerr saturation in this wavelength region.

Let us exemplify these considerations for argon. Our rigorous analysis clearly reveals that the infinite series for the nonlinear refractive index given by Eq. (1) converges. Yet, the series converges slowly, i.e., strictly speaking, we have to include some 100 terms in the series before the addition of even higher-order terms does not give further noticeable changes in the IDRI. Therefore a pure series representation of the intensity dependence appears rather impractical. However, we observe that the series of n_{2k} behaves like a geometric series for $k > 15$. Therefore we can exploit the geometric series property to estimate the contribution of the higher-order terms. This yields

$$\Delta n(I) = \sum_{k=1}^{k_0-1} n_{2k} I^k + \frac{n_{2k_0} I^{k_0}}{1 - I/I_{\text{conv}}}. \quad (29)$$

These results are visualized in Fig. 6. The red line represents the series Δn , truncated at $k_0 = 100$, while truncating at

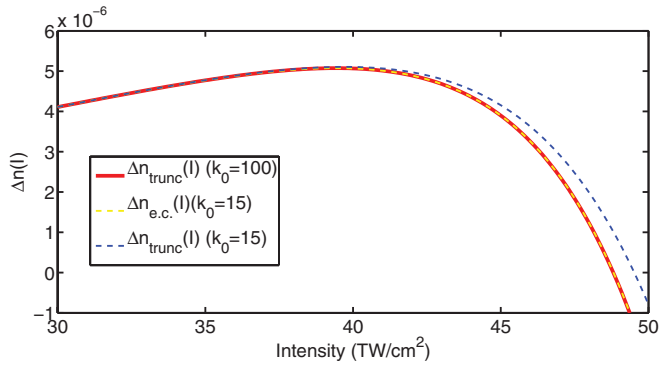


FIG. 6. (Color online) Comparison of truncated series representations of Eq. (1) and the geometric series representation. Red solid line: series truncated at $k = 100$. Blue dashed line: truncated at $k = 15$. Yellow dashed line: series truncated at $k = 15$, but augmented by correction term according to geometric series assumption Eq. (29).

$k_0 = 15$ yields the blue dashed line. While the latter may be suitable for most practical purposes, the curves start to deviate from each other above 45 TW/cm². Adding a geometric series correction term to Eq. (29) yields the yellow dashed curve, which is in excellent agreement with the full series representation (red line) in the depicted intensity range. Despite the slow convergence of the series for the nonlinear refractive index, it is therefore possible to consider only the first k_0 coefficients n_{2k} and adding an appropriate error correction as done in Eq. (29). We have checked that this works equally well for the other noble gases, and a table containing n_2 – n_{32} of the considered gases can be found in Refs. [17,42].

VII. CONCLUSIONS

We employed Kramers-Kronig theory to compute nonlinear refraction for all noble gases. Our theory is inherently simple, requiring knowledge of only a single parameter for prediction of n_2 and its dispersion for the entire transparency range of the gas. A detailed benchmark indicated excellent agreement of 10% to 20% with chemical reference data. Other than previous theoretical modeling, our method does not rely on any simplistic wavelength scaling arguments. Correctly predicting the expected sign change above the two-photon resonance, we therefore predict more reliable n_2 data in the ultraviolet. Moreover, by extending the formalism for computation of

the higher-order Kerr effect, we can model the recently observed saturation of the Kerr effect [21]. Again, our model calculations agree within reasonable accuracy with measured data.

It was recently suggested to monitor the ratio of the fifth and third harmonic, i.e., $\chi^{(5)}/\chi^{(3)}$, as an experimental test for the HOKE. In fact, such experiments reported a rather small ratio of the respective nonlinear susceptibilities, which was interpreted as an indication against a prominent role of the HOKE [43]. However, our Kramers-Kronig approach strongly suggests that the observed saturation behavior stems from much higher orders of the nonlinear susceptibility. For the case of argon, e.g., the observed saturation behavior goes back to nonlinear susceptibilities $\chi^{(21)}$ and above while the coefficients $\chi^{(5)}$ through $\chi^{(19)}$ do not contribute to the saturation. In fact, Kerr saturation much more resembles the appearance of the plateau region in high-harmonic generation [2]. Our approach therefore suggests the appearance intensity of a plateau in the harmonics for independent experimental verification.

Going significantly beyond previous publications [17,44], we further investigated the full dispersion of the saturation behavior and proved the convergence of our perturbational treatment down to Keldysh parameters close to unity. The wavelength dependence of the Kerr saturation corroborates the existence of two different filamentation scenarios. In the visible and ultraviolet, plasma formation is expected to arrest the collapse of the beam profile induced by self-focusing. However, this longstanding conceptual picture makes way for a novel scenario at longer wavelengths. Here the arrest of the collapse is induced by HOKE. We predict that these effects become particularly pronounced with the powerful new chirped-pulse optical parametric amplifier sources [12] currently emerging. Given that there is no dissipative mechanism necessary to confine the light in a small beam area, HOKE-based filaments open a completely new avenue of nonlinear optics with unprecedented nonlinear interaction lengths.

ACKNOWLEDGMENTS

Financial support from the Deutsche Forschungsgemeinschaft, Grants No. DE 1209/1-2 and No. STE 762/7-2, is gratefully acknowledged. G.S. gratefully acknowledges support from the Academy of Finland (Project Grant No. 128844).

[1] T. Brabec and F. Krausz, *Rev. Mod. Phys.* **72**, 545 (2000).
 [2] A. McPherson, G. Gibson, H. Jara, U. Johann, T. S. Luk, I. A. McIntyre, K. Boyer, and C. K. Rhodes, *J. Opt. Soc. Am. B* **4**, 595 (1987); X. F. Li, A. L'Huillier, M. Ferray, L. A. Lompré, and G. Mainfray, *Phys. Rev. A* **39**, 5751 (1989); P. B. Corkum, *Phys. Rev. Lett.* **71**, 1994 (1993).
 [3] M. Hentschel, R. Kienberger, C. Spielmann, G. A. Reider, N. Milosevic, T. Brabec, P. Corkum, U. Heinzmann, M. Drescher, and F. Krausz, *Nature (London)* **414**, 509 (2001).
 [4] M. Nisoli, S. De Silvestri, O. Svelto, R. Szipőcs, K. Ferencz, C. Spielmann, S. Sartania, and F. Krausz, *Opt. Lett.* **22**, 522 (1997).

[5] L. Bergé, S. Skupin, R. Nuter, J. Kasparian, and J.-P. Wolf, *Rep. Prog. Phys.* **70**, 1633 (2007).
 [6] C. V. Shank, R. L. Fork, R. Yen, R. H. Stolen, and W. J. Tomlinson, *Appl. Phys. Lett.* **40**, 761 (1982).
 [7] C. P. Hauri, W. Kornelis, F. W. Helbing, A. Heinrich, A. Couairon, A. Mysyrowicz, J. Biegert, and U. Keller, *Appl. Phys. B* **79**, 673 (2004).
 [8] A. Dubietis, G. Jonusauskas, and A. Piskarskas, *Opt. Commun.* **88**, 437 (1992); I. N. Ross, P. Matousek, M. Towrie, A. J. Langley, and J. L. Collier, *ibid.* **144**, 125 (1997); G. Cerullo, A. Baltuška, O. D. Mücke, and C. Vozzi, *Laser Phot. Rev.* **5**, 323 (2011).

- [9] Á. Börzsönyi, Z. Heiner, A. P. Kovács, M. P. Kalashnikov, and K. Osvay, *Opt. Express* **18**, 25847 (2010).
- [10] H. J. Lehmeier, W. Leupacher, and A. Penzkofer, *Opt. Commun.* **56**, 67 (1985).
- [11] M. Nurhuda, A. Suda, M. Hatayama, K. Nagasaka, and K. Midorikawa, *Phys. Rev. A* **66**, 023811 (2002).
- [12] G. Andriukaitis *et al.*, *Opt. Lett.* **36**, 2755 (2011).
- [13] T. Nagy and P. Simon, *Opt. Lett.* **34**, 2300 (2009).
- [14] R. C. Miller, *Appl. Phys. Lett.* **5**, 17 (1964).
- [15] D. M. Bishop, *Phys. Rev. Lett.* **61**, 322 (1988).
- [16] J. Seres, *Appl. Phys. B* **73**, 705 (2001).
- [17] C. Brée, A. Demircan, and G. Steinmeyer, *Phys. Rev. Lett.* **106**, 183902 (2011).
- [18] M. Sheik-Bahae, D. J. Hagan, and E. W. Van Stryland, *Phys. Rev. Lett.* **65**, 96 (1990).
- [19] M. Sheik-Bahae, D. C. Hutchings, D. J. Hagan, and E. W. Van Stryland, *IEEE J. Quantum Electron.* **27**, 1296 (1991).
- [20] S. V. Popruzhenko, V. D. Mur, V. S. Popov, and D. Bauer, *Phys. Rev. Lett.* **101**, 193003 (2008).
- [21] V. Loriot, E. Hertz, O. Faucher, and B. Lavorel, *Opt. Express* **17**, 13429 (2009); **18**, 3011(E) (2010).
- [22] D. C. Hutchings, M. Sheik-Bahae, D. J. Hagan, and E. W. Van Stryland, *Opt. Quantum Electron.* **24**, 1 (1992).
- [23] H. A. Kramers, *Atti Cong. Intern. Fisica*, **2**, 545 (1927).
- [24] R. de L. Kronig, *J. Opt. Soc. Am.* **12**, 547 (1926).
- [25] B. S. Wherrett, *J. Opt. Soc. Am. B* **1**, 67 (1984).
- [26] L. V. Keldysh, *Sov. Phys. JETP* **20**, 1307 (1965).
- [27] A. M. Perelomov, V. S. Popov, and M. V. Terent'ev, *Sov. Phys. JETP* **23**, 924 (1966).
- [28] D. P. Shelton and J. E. Rice, *Chem. Rev.* **94**, 3 (1994).
- [29] M. J. Shaw, C. J. Hooker, and D. C. Wilson, *Opt. Commun.* **103**, 153 (1993).
- [30] D. M. Bishop and J. Pipin, *J. Chem. Phys.* **91**, 3549 (1989).
- [31] J. E. Rice, *J. Chem. Phys.* **96**, 7580 (1992).
- [32] T. Lundeen, S.-Y. Hou, and J. W. Nibler, *J. Chem. Phys.* **79**, 6301 (1983).
- [33] T. Kobayashi, K. Sasagane, and K. Yamaguchi, *J. Chem. Phys.* **112**, 7903 (2000).
- [34] P. Fuentealba and O. Reyes, *J. Phys. B* **26**, 2245 (1993).
- [35] Y. Malykhanov, I. Eremkin, and S. Begeeva, *J. Appl. Spectrosc.* **75**, 1 (2008).
- [36] C. Lupinetti and A. J. Thakkar, *J. Chem. Phys.* **122**, 044301 (2005).
- [37] M. Nurhuda, A. Suda, and K. Midorikawa, *New J. Phys.* **10**, 053006 (2008).
- [38] D. S. Steingrube, E. Schulz, T. Binhammer, M. B. Gaarde, A. Couairon, U. Morgner, and M. Kovacev, *New J. Phys.* **13**, 043022 (2011).
- [39] M. Nurhuda, A. Suda, and K. Midorikawa, *RIKEN Rev.* **48**, 40 (2002).
- [40] V. Loriot, P. Béjot, W. Ettoumi, Y. Petit, J. Kasparian, S. Henin, E. Hertz, B. Lavorel, O. Faucher, and J. P. Wolf, *Laser Phys.* **21**, 1319 (2011).
- [41] F. W. J. Olver, D. W. Lozier, R. F. Boisvert, and C. W. Clark, eds., *NIST Handbook of Mathematical Functions* (Cambridge University Press, Cambridge, UK, 2010).
- [42] C. Brée, A. Demircan, and G. Steinmeyer, *Phys. Rev. Lett.* **106**, 183902 (2011) (see supplementary material for a compilation of the nonlinear coefficients n_2 to n_{32} of He, Ne, Ar, Kr, and Xe).
- [43] G. O. Ariunbold, P. Polynkin, and J. V. Moloney, *Opt. Express* **20**, 1662 (2012).
- [44] C. Brée, A. Demircan, and G. Steinmeyer, *IEEE J. Quantum Electron.* **46**, 433 (2010).